

Control of Circular Cylinder Flow by the Use of Dimples

P. W. Bearman* and J. K. Harvey†

Imperial College of Science, Technology and Medicine, London SW7 2BY, England, United Kingdom

Measurements are reported of the drag coefficient and Strouhal number of a dimpled circular cylinder over the Reynolds number range from 2×10^4 to 3×10^5 . The ratio of the depth of the dimples to the diameter of the cylinder is 9×10^{-3} . In common with sand-roughened cylinders, the dimpled cylinder has a lower critical Reynolds number than a smooth cylinder. After the drag coefficient minimum, the C_D does not rise to the high values that are typical of cylinders with sand roughness but is found to be closer to that for a smooth cylinder. Over a Reynolds number range from about 4×10^4 to 3×10^5 , a dimpled circular cylinder has a lower drag coefficient than a smooth cylinder.

Introduction

A CIRCULAR cylinder generates a high mean drag and large fluctuating forces. Over the last 40 years or so a considerable number of investigations have been carried out to study ways of reducing these forces, either by controlling the flow passively or by using some form of active control. Among the passive control devices that have been studied are wake splitter plates¹ and perforated shrouds.² The latter device has been used to suppress flow-induced vibration of cylinders caused by the regular shedding of vortices. The fitting of helical strakes³ is another means of reducing the vibration levels of circular cylinders excited by vortex shedding. However, a major disadvantage of using strakes is that they increase the drag force above the equivalent value for a plain cylinder. This increase is particularly large at postcritical Reynolds numbers. Perforated shrouds are interesting in that they reduce the drag coefficient, relative to a plain cylinder, at subcritical Reynolds numbers but they increase it at postcritical values.

There is a broad range of Reynolds number, spanning the transition between the subcritical and postcritical regimes and stretching far above it, where the flow around a circular cylinder can be influenced significantly by increasing the roughness of its surface. For a cylinder with a smooth surface, placed in a low-turbulence level stream, the start of the drag coefficient fall, marking the beginning of the critical regime, occurs at a Reynolds number of around 3×10^5 . At Reynolds numbers below this value, the application of an appropriate degree of surface roughness can be a very effective means of reducing the drag coefficient. However, as shown by Achenbach,⁴ the reduction in C_D for a rough cylinder as the Reynolds number is increased through the critical regime is less than that for one with a smooth surface. In general, the rougher the cylinder surface, the lower the value of the critical Reynolds number, but the smaller the fall in C_D through the critical regime. Achenbach also showed that in the high Reynolds number postcritical regime a cylinder with a rough surface finish has a higher drag coefficient than one with a smooth surface.

The flow around a sphere depends on surface roughness in a manner very similar to the way roughness affects the flow around a circular cylinder. As part of an investigation into the aerodynamics of golf balls, Bearman and Harvey⁵ compared their measurements of the variation of C_D with Reynolds number for a dimpled golf ball with measurements of Achenbach⁶ for spheres with sand-grain roughness. The comparison is reproduced in Fig. 1. Achenbach carried out a series of experiments for spheres with various ratios of the average diameter

of the sand grains k to the sphere diameter D . It can be seen from Fig. 1 that, for sand-roughened spheres, increasing k/D reduces the Reynolds number for the drag coefficient fall but that after the minimum the C_D increases rapidly again with increasing Reynolds number. The increased C_D with increased surface roughness in the postcritical regime is thought to be due mainly to the effect of the roughness on the development of the turbulent boundary layer growing on the sphere. Compared with a smooth surface, the roughness causes a thickening of the boundary layer, which leads to an earlier separation of the flow. Equating k to the depth of the dimples on a golf ball, then for a typical golf ball the corresponding value of k/D is 9×10^{-3} . For similar values of k/D , the results in Fig. 1 suggest that dimples cause the C_D to fall at a lower Reynolds number than for a sand-roughened sphere. Also it is evident that after this fall the drag coefficient remains almost constant at about 0.25 for the golf ball, whereas for the sand-roughened sphere it rises sharply after the minimum and asymptotes to a value of about 0.4. Hence, by considering drag coefficient values, it appears that in the postcritical regime the dimples have a more beneficial effect on the flow development than sand roughness.

The present paper describes the results of experiments to assess the effect of dimples on the flow around a circular cylinder as it undergoes transition from subcritical to postcritical flow. The main aim of the investigation was to determine whether dimples can be used to control the flow in the same way as on a sphere. This paper has been prompted by a recent experimental and computational study reported by Kimura and Tsutahara⁷ on the effect of spanwise grooves on the flow around a circular cylinder. The width and depth of the grooves, relative to the diameter of the cylinder, were chosen to be similar to the diameter and depth of dimples on a golf ball. In their experiments, which were carried out at a Rey-

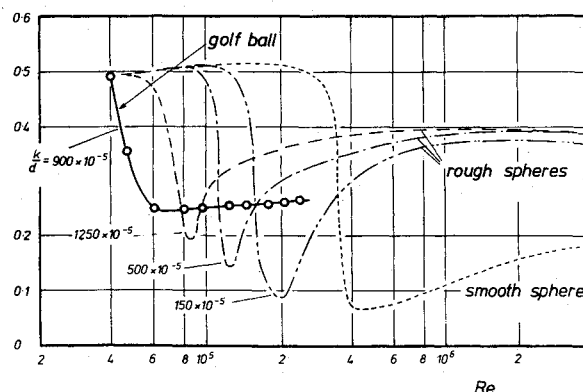


Fig. 1 Variation of C_D with Reynolds number for smooth and sand-roughened spheres and a golf ball.

Received June 9, 1992; revision received Jan. 27, 1993; accepted for publication Feb. 1, 1993. Copyright © 1993 by the American Institute of Aeronautics and Astronautics, Inc. All rights reserved.

*Professor and Head, Department of Aeronautics. Member AIAA.

†Professor, Department of Aeronautics. Member AIAA.

nolds number of 2.2×10^3 , just one groove was cut into the cylinder. By rotating the cylinder it was found that separation could be delayed by a few degrees on the side with the groove if the groove was located at approximately 80 deg from the front stagnation point. In addition, they computed the flow around a circular cylinder with a single groove on each side, at a Reynolds number of 1.2×10^3 , and also found a slight delay in boundary-layer separation when the grooves were set at about 80 deg. They speculate that their findings help to explain why the dimples on a golf ball are more efficient at reducing drag than sand roughness.

The effect of circumferential grooves on the drag of axisymmetric bluff bodies had been studied earlier by Howard and Goodman.⁸ They also found that the grooves produced a reduction in drag. Kimura and Tsutahara argue that the flow near the wall is more energetic just downstream of a groove or shallow cavity and that therefore the boundary layer can travel slightly farther against an adverse pressure gradient before separating. The position of the groove is critical, however, because if the flow should fail to reattach at the downstream end of the groove, then separation of flow from the cylinder could be advanced instead. They suggest that the grooves will be effective at delaying separation at higher Reynolds numbers and also when there is a turbulent boundary layer on the cylinder. However, in any practical application it will be very difficult to arrange for the grooves to be orientated in precisely the correct positions to delay separation. Hence, to use this technique, it is likely that a regular distribution of longitudinal grooves would have to be cut into the cylinder surface. It is not known, however, whether this type of surface would have any better aerodynamic characteristics than a sand-roughened cylinder.

Although there are differences between the flow in a two-dimensional groove and the flow in a dimple, we thought it would be interesting to present our measurements for a dimpled cylinder. In the experiment to be described we measured the drag and the vortex-shedding frequency of a circular cylinder into which was machined an array of dimples similar to those on a golf ball.

Experimental Arrangement

Experiments were carried out in a low-speed wind tunnel with a closed test section 1.37 m wide by 1.22 m high. The freestream turbulence level in the tunnel was less than 0.2%, and the mean flow was uniform to around $\pm 1\%$. A circular cylinder with a diameter of 9.95 cm was mounted horizontally across the test section. The cylinder surface was machined to give rows of dimples across the span as shown in Fig. 2. Twelve equally spaced dimples with a depth of 0.91 mm were machined around the circumference of the cylinder. The dimples were shaped using a spherical cutter, and since they were formed on a cylinder, they appear as ellipses. The major axis, which is along the cylinder span, was 11.15 mm, and the minor

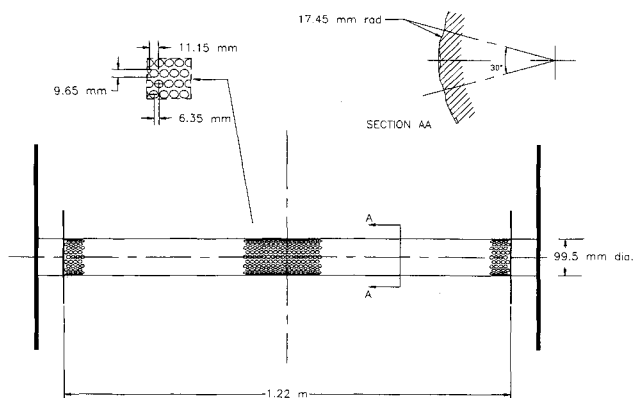


Fig. 2 Sketch showing details of the dimples.

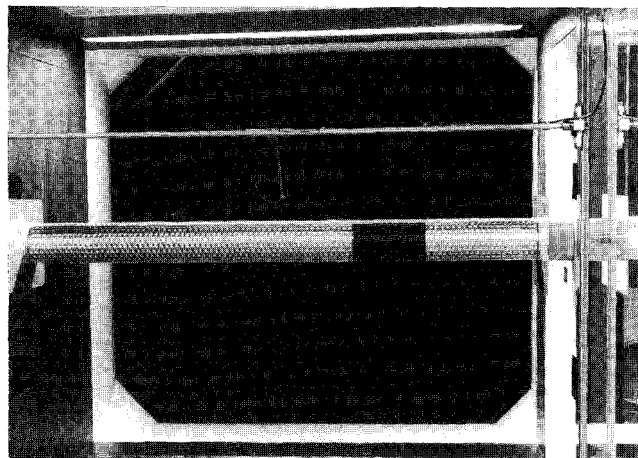


Fig. 3 Dimpled circular cylinder mounted in the wind tunnel.

axis was 9.65 mm. This pattern was repeated in steps of 6.35 mm across the cylinder span, with every other set of dimples rotated in the circumferential direction by half a dimple spacing, so as to give a staggered arrangement. The density of the dimples was such that 180 were machined into a length of the cylinder equal to just under its diameter. The plan area of each dimple was about 50% greater than the corresponding scaled area of a dimple on a conventional golf ball, and the density of dimples was half that of a normal golf ball.

By rotating the cylinder about its axis, we can place the dimples in a variety of orientations to the oncoming flow. In this investigation, the majority of the experiments were carried out with the cylinder aligned such that a row of dimples was placed symmetrically either side of the foremost part of the cylinder. However, some measurements were made with the centers of dimples at the front of the cylinder. Unless stated otherwise, it can be assumed that the measurements reported were made with the cylinder in the former orientation.

The dimpled cylinder was connected by rods to arms outside the tunnel that were attached in turn to the wind-tunnel balance. A view of the cylinder in the tunnel is shown in Fig. 3. The drag was measured on a section of cylinder 1.22 m long and fitted with thin end plates 20 cm wide. The aspect ratio of the cylinder between the end plates was 12.26. Outside the end plates the supporting rods passed through dummy cylinder sections connected to the tunnel walls. The vortex-shedding frequency n was measured from the velocity signal obtained from a hot-wire probe placed outside the cylinder wake at a distance behind the cylinder equal to about a cylinder diameter. The shedding frequency measurements are presented as Strouhal number S where $S = nD/U$ and U is flow speed. With the cylinder in the test section, the maximum flow speed was about 42 m/s, and this corresponds to a Reynolds number Re of around 3×10^5 . The geometric blockage caused by the model in the tunnel was 8.2%, and corrections were made to the measured velocity by applying the method of Allen and Vincenti.⁹ Corrected velocities were used to calculate Re , S , and C_D .

Experimental Results

Measurements of C_D vs Re for a dimpled circular cylinder are plotted in Fig. 4. Also shown are results for a smooth cylinder, due to Wieselberger,¹⁰ and measurements of Achenbach⁴ for a sand-roughened cylinder with $k/D = 4.5 \times 10^{-3}$ and 9×10^{-3} . Over a range of Re from 2×10^4 to 4×10^4 the C_D values for the smooth and dimpled cylinders are in close agreement. The minimum value of C_D for the dimpled cylinder occurs at about $Re = 10^5$, and at the highest Reynolds numbers tested the drag coefficient appears to be approaching asymptotically a value a little above 0.7. A further set of measurements of C_D vs Re was made with the cylinder rotated through an angular distance

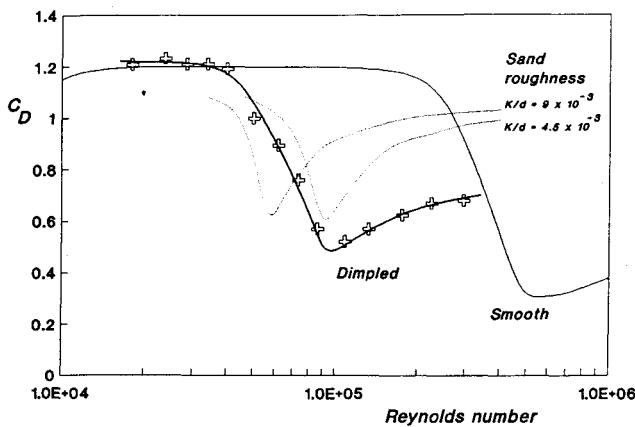


Fig. 4 Variation of C_D with Reynolds number for smooth,¹⁰ sand-roughened,⁴ and dimpled circular cylinder.

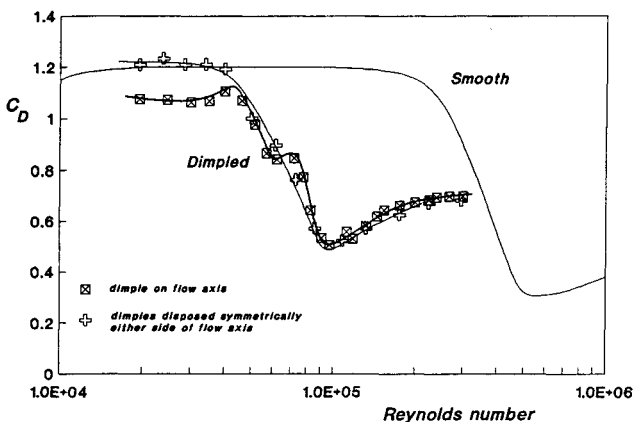


Fig. 5 Variation of C_D with Reynolds number for two orientations of the dimples.

corresponding to half a dimple spacing so that the centers of dimples faced the oncoming flow. A comparison of these results with those obtained with the cylinder in its original orientation is shown in Fig. 5. A marked difference in C_D is observed at subcritical Reynolds numbers, with lower drag recorded when dimples faced the flow, but at the highest values of Re examined the two sets of results are in much closer agreement. A plateau in the variation of C_D with Re is seen to occur between $Re = 6 \times 10^4$ and 7×10^4 .

Measurements of Strouhal number plotted against Reynolds number for a smooth and a dimpled cylinder are shown in Fig. 6. The smooth cylinder values of S are due to Bearman¹¹ and show the characteristic variation of S with Re in the critical regime above $Re = 3 \times 10^5$ as first one separation bubble forms on the cylinder and then the second one forms on the opposite side. The variation of S with Re for the dimpled cylinder mirrors the variation of C_D with Re . At low Re the Strouhal number corresponds to that for a smooth cylinder, and at high Re it approaches a value just above 0.25. In between, it reaches a maximum at about the same Reynolds number as C_D falls to its minimum value.

Discussion of Results

If, as for the golf ball, the roughness height k for the dimpled cylinder is taken as the depth of the dimples, then $k/D = 9.1 \times 10^{-3}$. Comparing C_D values with those for a sand-roughened cylinder with a similar value of k/D shows that sand roughness induces the fall in C_D at a lower value of Re , although the dimples cause the larger reduction. In the case of the sphere experiments,⁵ it was the golf ball that experienced the earlier fall for a matching value of k/D . However, in agreement with the golf ball measurements, the dimpled cylin-

der drag coefficient at high values of Re is substantially less than that of the sand-roughened one. At the highest value of Re investigated, the C_D for the dimpled cylinder approached a value close to that for a smooth cylinder in the postcritical regime.

The variation of Strouhal number with Re for the dimpled cylinder through the critical Reynolds number regime shows a much smaller value of S , compared with a smooth cylinder, at the Reynolds number where the C_D is a minimum. The level of S at the highest Re value examined is close to the postcritical value for a smooth cylinder. It is interesting to note that for the dimpled cylinder vortex shedding remained strong and regular throughout the Reynolds number range examined. It did not exhibit the weak and irregular shedding that is a characteristic of part of the Reynolds number range spanning the transition from subcritical to postcritical flow for a smooth cylinder.¹¹ It is tempting to hypothesize that by applying dimples to model chimneys, for instance, full-scale flow conditions could be simulated at Reynolds numbers as low as 3×10^5 .

Some attempts were made to examine the flow generated by the dimples by using the surface oil flow technique and by traversing a hot-wire probe just downstream of a dimple. The small scale of the flow features being studied made it very difficult to draw many definite conclusions. However, it is thought that a pair of vortices trails back from each dimple and that these vortices may help to energize the cylinder's boundary layer. The disturbance introduced by a dimple promotes transition, and it is likely that, at a particular Reynolds number, transition occurs at a fixed angular position across the span of the cylinder. Similarly, separation is very likely to be fixed by a line of dimples along the cylinder span. A surface oil flow picture is shown in Fig. 7, and it can be seen that there is a straight separation line across the region of flow visualized. The flow is from top to bottom, and the separation occurs close to the 90-deg point on the cylinder. An intricate

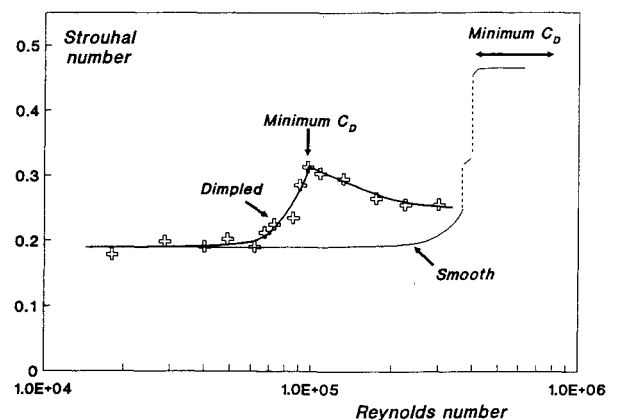


Fig. 6 Variation of Strouhal number with Reynolds number for a smooth¹¹ and a dimpled circular cylinder (+).

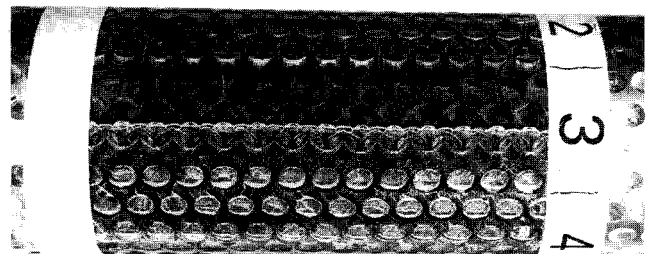


Fig. 7 Surface oil flow visualization on a dimpled circular cylinder; flow from top to bottom.

surface flow pattern is observed just downstream of separation with structures appearing to be linked between adjacent spanwise dimples.

It is clear from Fig. 5 that the orientation of the dimples to the approaching flow has some influence on C_D . The effect is seen mainly in the subcritical regime where it is expected that the cylinder's boundary layer is laminar and that separation occurs around 80 deg. As observed in the experiments of Kimura and Tsutahara, separation may occur at the front of a groove or be delayed until a little way after it, depending on its orientation. Dimples may influence the cylinder flow in a similar way. The reason for the small plateau in C_D observed in the results plotted in Fig. 4 is not clear. It is not thought to be due to the formation of a separation bubble because it is difficult to understand how a two-dimensional bubble could exist across a dimpled cylinder. It is more likely to be due to separation being fixed at perhaps the front of a particular line of dimples.

Conclusions

Experiments carried out on a dimpled circular cylinder show that dimples cause the critical regime to occur at a lower Reynolds number than that for a smooth cylinder. The values of C_D measured in the postcritical regime are very close to those for a smooth cylinder in postcritical flow, and they do not attain the high values that are typical of sand-roughened cylinders. It appears that dimples affect the flow around a circular cylinder in a similar manner to the way that dimples influence the flow around a golf ball. The dimples used were modeled on those found on a typical golf ball, and no attempt was made to optimize their dimensions. It is possible that larger reduc-

tions in drag could be obtained with another design of dimple or with a different arrangement of dimples.

References

- ¹Roshko, A., "On the Drag and Shedding Frequency of Two-Dimensional Bluff Bodies," NACA TN 3169, 1954.
- ²Price, P., "Suppression of the Fluid-Induced Vibrations of Circular Cylinders," *Proceedings of the American Society of Civil Engineers*, EM3, 1954, p. 1030.
- ³Walshe, D. E. J., *Wind-Excited Oscillations of Structures*, Her Majesty's Stationary Office, London, 1972.
- ⁴Achenbach, E., "Influence of Surface Roughness on the Cross-Flow Around a Circular Cylinder," *Journal of Fluid Mechanics*, Vol. 46, Pt. 2, 1971, pp. 321-335.
- ⁵Bearman, P. W., and Harvey, J. K., "Golf Ball Aerodynamics," *Aeronautical Quarterly*, May 1976, pp. 112-122.
- ⁶Achenbach, E., "The Effects of Surface Roughness and Tunnel Blockage on the Flow Past Spheres," *Journal of Fluid Mechanics*, Vol. 65, Pt. 1, 1974, pp. 113-125.
- ⁷Kimura, T., and Tsutahara, T., "Fluid Dynamic Effects of Grooves on Circular Cylinder Surface," *AIAA Journal*, Vol. 29, No. 12, 1991, pp. 2062-2068.
- ⁸Howard, F. G., and Goodman, W. L., "Axisymmetric Bluff-Body Drag Reduction Through Geometrical Modification," *Journal of Aircraft*, Vol. 22, No. 6, 1985, pp. 516-522.
- ⁹Allen, H. J., and Vincenti, W. G., "Wall Interference in a Two-Dimensional-Flow Wind Tunnel, with Consideration of the Effect of Compressibility," NACA Rept. 782, 1944.
- ¹⁰Wieselberger, C., "Neuere Feststellungen über die Gesetze des Flüssigkeits- und Luftwiderstands," *Physikalische Zeitschrift*, Vol. 22, 1921, pp. 321-328.
- ¹¹Bearman, P. W., "On Vortex Shedding from a Circular Cylinder in the Critical Reynolds Number Regime," *Journal of Fluid Mechanics*, Vol. 34, 1969, pp. 577-585.

Recommended Reading from Progress in Astronautics and Aeronautics

UNSTEADY TRANSONIC AERODYNAMICS

David Nixon, editor



1989, 385 pp, illus, Hardback
ISBN 0-930403-52-5
AIAA Members \$52.95
Nonmembers \$69.95
Order #: V-120 (830)

Unsteady transonic aerodynamics is a field with many differences from its counterpart, steady aerodynamics. The first volume of its kind, this timely text presents eight chapters on Physical Phenomena Associated with Unsteady Transonic Flows; Basic Equations for Unsteady Transonic Flow; Practical Problems: Airplanes; Basic Numerical Methods; Computational Methods for Unsteady Transonic Flow; Application of Transonic Flow Analysis to Helicopter Rotor Problems; Unsteady Aerodynamics for Turbomachinery Aeroelastic Applications; and Alternative Methods for Modeling Unsteady Transonic Flows. Includes more than 470 references, 180 figures, and 425 equations.

Sales Tax: CA residents, 8.25%; DC, 6%. For shipping and handling add \$4.75 for 1-4 books (call for rates for higher quantities). Orders under \$100.00 must be prepaid. Foreign orders must be prepaid and include a \$20.00 postal surcharge. Please allow 4 weeks for delivery. Prices are subject to change without notice. Returns will be accepted within 30 days. Non-U.S. residents are responsible for payment of any taxes required by their government.

Place your order today! Call 1-800/682-AIAA



American Institute of Aeronautics and Astronautics

Publications Customer Service, 9 Jay Gould Ct., P.O. Box 753, Waldorf, MD 20604
FAX 301/843-0159 Phone 1-800/682-2422 9 a.m. - 5 p.m. Eastern